Available online at www.sciencedirect.com
SCIENCE DIRECT®
International Journal of Thermal Sciences 43 (2004) 165–171
International Journal of Thermal Sciences
www.elsevier.com/locate/ijts

Thermal behavior of thin slab as described by the parabolic microscopic heat conduction model with variable thermal properties

Moh'd A. Al-Nimr *, Malak Naji, Salem A. Al-Wardat

Mechanical Engineering Department, Jordan University of Science and Technology, Irbid 22110, P.O. Box 3030, Jordan

Received 5 March 2003; accepted 19 May 2003

Abstract

The thermal behavior of thin slab as described by the parabolic microscopic heat conduction model with variable thermal properties is investigated under two types of heating sources. These types are the unit step and the fluctuating harmonic heating sources. The considered thermal properties are the electron gas C_e and the solid lattice C_L total thermal capacities. It is found that the slab thermal behavior is more sensitive to the variation in C_e as compared to the variation in C_L. Assuming C_e constant may cause an error of magnitude 19% while assuming C_L constant causes an error of magnitude 5%. The sensitivity of the parabolic microscopic heat conduction model to the variation in C_e is higher under the effect of a fluctuating heating source as compared to a unit step heating source.

Keywords: Parabolic microscopic model; Parabolic two step conduction model; Microscopic heat conduction model; Conduction with variable thermal properties; Microscopic model with variable thermal properties; Variable total thermal capacity; Two-step model with variable properties

1. Introduction

High-rate heating of thin metal films is a rapidly emerging area in heat transfer [1–13]. When a thin film is exposed to a very rapid heating process such that induced by a short-pulse laser, the typical response time for the film is an order of picoseconds, which is comparable to the phonon–electron thermal relaxation time. Under these situations, thermal equilibrium between solid lattice and electron gas cannot be assumed and heat transfer in the electron gas and the metal lattice needs to be considered separately. Models describing the non-equilibrium thermal behavior in such cases are called the microscopic two-step models. Two microscopic heat conduction models are available in the literature. The first one is the parabolic two-step model [1–5, 8–10] and the second one is the hyperbolic two-step model [1,3,7,11].

Ultrafast heating of metals consists of two major steps of energy transfer, which occur simultaneously. In the first step electrons absorb most of the incident radiation energy and the excited electron gas transmits its energy to the lattice through inelastic electron–phonon scattering process [1,3]. In the second step, the incident radiation absorbed by the metal film diffuses spatially within the film mainly by the electron gas. For typical metals, depending on the degree of electron–phonon coupling, it takes about 0.1 to 1 picosecond for electrons and lattice to reach thermal equilibrium. When the ultrafast heating pulse duration is comparable with or less than this thermalization time, electrons and lattice are not in thermal equilibrium. As a result, the thermal behavior of the thin film under the effect of the microscopic parabolic heat conduction model is describe by [1,3]

$$C_e(T_e)\frac{\partial T_e}{\partial t} = \nabla\cdot(k_e\nabla T_e) - G(T_e - T_L) + S_e \tag{1}$$

$$C_L(T_L)\frac{\partial T_L}{\partial t} = G(T_e - T_L) \tag{2}$$

where C_L denotes the lattice heat capacity, C_e the electron heat capacity, T_L the lattice temperature, T_e the electron temperature, k_e the electron thermal conductivity, t the time, ∇ the gradient vector, S_e the heating source within the electron gas and G denotes the coupling factor which characterizes the energy exchange between phonons and electrons. Eqs. (1) and (2) represent the parabolic microscopic heat conduction model which implies that the electron and lattice temperatures are not in local thermal equilibrium, i.e., $T_e \neq T_L$. If electron gas and solid lattice are in local thermal equilibrium, i.e., $T_e = T_L$, then the parabolic microscopic

* Corresponding author.
E-mail address: malnimr@just.edu.jo (M.A. Al-Nimr).

1290-0729/$ – see front matter
doi:10.1016/j.ijthermalsci.2003.05.001

Nomenclature

C	heat capacity	$J\cdot m^{-3}\cdot K^{-1}$
G	electron–phonon coupling factor	$W\cdot m^{-3}\cdot K^{-1}$
K	thermal conductivity	$W\cdot m^{-1}\cdot K^{-1}$
L	film thickness	m
s	Laplacian domain	
S_e	heating source per unit volume, $= S_0(1+\varepsilon\sin(\bar{w}t))$	
S_0	amplitude of volumetric heating source	$W\cdot m^{-3}$
S	dimensionless volumetric heat source, $= S_e/S_0$	
t	time	s
t_0	pulse duration	s
T	temperature	K
T_i	initial temperature	K

Greek symbols

ε	amplitude of fluctuation
η	dimensionless time, $= \alpha t/L^2$
η_0	dimensionless pulse duration, $= \alpha t_0/L^2$
Θ	Laplace transformation of θ
θ	dimensionless temperature, $= (T-T_i)/T_i$
ω	dimensionless angular velocity of the fluctuating heat source, $= \bar{w}L^2/\alpha$
$\bar{w}$	angular velocity of the fluctuating volumetric heat source ..... $rad\cdot s^{-1}$

Subscripts

e	electron
L	lattice
i	initial

heat conduction model reduces to the parabolic macroscopic (Fourier) heat conduction model.

Using different solving techniques, the microscopic parabolic heat conduction model has been used numerously to describe the thermal behavior of thin metal films under different applications, operating conditions, geometrical parameters and metal properties. In the previous solutions of the two-step models the material thermophysical properties are assumed to be constant which simplify the solution. In this work we take into consideration the material properties dependency on temperature and in order to rigorously account for the temperature dependence of material properties the microscopic parabolic two-step model must be solved numerically.

2. Analysis

2.1. Variable thermal properties

Consider a thin metal slab of thickness L which is exposed to an incident volumetric radiative heating source. Two types of volumetric heating sources are considered which are the unit step and the harmonic types. The incident radiation is assumed to be totally absorbed by the electron gas and the slab is assumed thermally insulated from both sides during the heating process. Also, the slab thermal behavior is assumed to be lumped in which the slab temperature is independent on the location. Taking into consideration the temperature dependence of the thermal properties, the parabolic microscopic heat conduction model is given as

$$C_e(T_e)\frac{\partial T_e}{\partial t} = -G(T_e - T_L) + S_e(t) \tag{3}$$

$$C_L(T_L)\frac{\partial T_L}{\partial t} = G(T_e - T_L) \tag{4}$$

While G is assumed to be constant. Eqs. (3) and (4) represent the parabolic microscopic heat conduction model which implies that the electron and lattice temperatures are not in local thermal equilibrium, i.e., $T_e \neq T_L$. Also,

$$C_e(T_e) = \gamma T_e \tag{5}$$

$$C_L(T_L) = a + b\cdot T_L + c\cdot T_L^2 + d\cdot T_L^3 \tag{6}$$

Eqs. (5) and (6) are obtained as correlation's for available experimental data for many metals over a wide range of temperatures and the values of γ are given by Kittel [14]. Eq. (6) governs the most general behavior of C_L with respect to temperature and many special cases may be obtained from it. As an example, under very low operating temperatures (a, b and c) may be set to zero and as a result, $C_L = d\cdot T_L^3$, which is the known formula for C_L of metals at low temperatures. Eqs. (3) and (4) assume the following initial conditions:

$$T_e(0) = T_L(0) = T_i \tag{7}$$

Combining Eqs. (7) and (4), two initial conditions in terms of T_L are given as

$$T_L(0) = T_i, \qquad \frac{\partial T_L}{\partial t}(0) = 0 \tag{8}$$

Eqs. (3) to (6) are combined to yield the following equations in terms of T_L:

$$F_1(T)\frac{\partial T}{\partial t} + F_2(T)\left(\frac{\partial T}{\partial t}\right)^2 + F_3(T)\left(\frac{\partial T}{\partial t}\right)^3 + F_4(T)\left(\frac{\partial^2 T}{\partial t^2}\right) + F_5(T)\frac{\partial T}{\partial t}\frac{\partial^2 T}{\partial t^2} = S_e \tag{9}$$

where

$$F_1(T) = a + (b+\gamma)T + cT^2 + dT^3$$

$$F_2(T)=\left(\frac{\gamma}{G}\right)\left[\left(bT+2cT^2+3dT^3\right)+\left(a+bT+cT^2+dT^3\right)\right]$$

$$F_3(T)=\left(\frac{\gamma}{G^2}\right)\left[\left(a+bT+cT^2+dT^3\right)\times\left(b+2cT+3dT^2\right)\right]$$

$$F_4(T)=\left(\frac{\gamma}{G}\right)\left[aT+bT^2+cT^3+dT^4\right]$$

$$F_5(T)=\left(\frac{\gamma}{G^2}\right)\left[a+bT+cT^2+dT^3\right]^2$$

where $T\equiv T_L$, with the subscript "L" is omitted for the sake of convenience. Now, using the dimensionless parameters defined in the Nomenclature, Eq. (9) are rewritten as:

$$F_1(\theta)\frac{\partial\theta}{\partial\eta}+F_2(\theta)\left(\frac{\partial\theta}{\partial\eta}\right)+F_3(\theta)\left(\frac{\partial\theta}{\partial\eta}\right)^3+F_4(\theta)\frac{\partial^2\theta}{\partial\eta^2}+F_5(\theta)\frac{\partial\theta}{\partial\eta}\frac{\partial^2\theta}{\partial\eta^2}=S\cdot S_0 \tag{10}$$

where

$$F_1(\theta)=\left(\frac{T_i}{t_0}\right)\left(a+(b+\gamma)T_i(1+\theta)+cT_i^2(1+\theta)+dT_i^3(1+\theta)^3\right)$$

$$F_2(\theta)=\left(\frac{\gamma T_i^2}{Gt_0^2}\right)\left[\left(bT_i(1+\theta)+2cT_i^2(1+\theta)^2+3dT_i^3(1+\theta)^3\right)+\left(a+bT_i(1+\theta)+cT_i^2(1+\theta)^2+dT_i^3(1+\theta)^3\right)\right]$$

$$F_3(\theta)=\left(\frac{\gamma T_i^3}{G^2t_0^3}\right)\left[\left(a+bT_i(1+\theta)+cT_i^2(1+\theta)^2+dT_i^3(1+\theta)^3\right)\times\left(b+2cT_i(1+\theta)+3dT_i^2(1+\theta)^2\right)\right]$$

$$F_4(\theta)=\left(\frac{\gamma T_i}{Gt_0^2}\right)\left(aT_i(1+\theta)+bT_i^2(1+\theta)^2+cT_i^3(1+\theta)^3+dT_i^4(1+\theta)^4\right)$$

$$F_5(\theta)=\left(\frac{\gamma T_i^2}{G^2t_0^3}\right)\left(a+bT_i(1+\theta)+cT_i^2(1+\theta)^2+dT_i^3(1+\theta)^3\right)^2$$

and the initial conditions become:

$$\theta(0)=0,\qquad \frac{\partial\theta}{\partial\eta}(0)=0 \tag{11}$$

2.2. Constant thermal properties

In this special case, C_e, C_L and G are assumed constant and as a result, the governing equations are given as:

$$C_e=\frac{\partial T_e}{\partial t}=-G(T_e-T_L)+S_e \tag{12}$$

$$C_L=\frac{\partial T_L}{\partial t}=-G(T_e-T_L) \tag{13}$$

$$T_e(0)=T_L(0)=T_i \tag{14}$$

Eqs. (13) and (14) may be combined to yield two initial conditions in terms of T_L as:

$$T_L(0)=T_i,\qquad \frac{\partial T_L}{\partial t}(0)=0 \tag{15}$$

Eqs. (12) and (13) are combined to yield:

$$\frac{\partial^2T}{\partial t^2}+C_1\frac{\partial T}{\partial t}=C_2S_e \tag{16}$$

with

$$C_1=\frac{G(C_e+C_L)}{C_eC_L},\qquad C_2=\frac{G}{C_eC_L}$$

where $T\equiv T_L$, with the subscript "L" is omitted for the sake of convenience. Eqs. (15) and (16) are rewritten in dimensionless form as:

$$\frac{\partial^2\theta}{\partial\eta^2}+C_3\frac{\partial\theta}{\partial\eta}=C_4S \tag{17}$$

$$\theta(0)=0,\qquad \frac{\partial\theta}{\partial\eta}(0)=0 \tag{18}$$

with

$$C_3=\frac{C_1L^2}{\alpha},\qquad C_4=\frac{C_2L^4S_0}{T_i\alpha^2}$$

2.3. Heating sources

The two heating sources, considered in the present work are described as:

2.3.1. Unit step heating source

The unit step volumetric heating source has the following dimensionless form:

$$S(\eta)=\left[1-u(\eta-\eta_0)\right]$$

where $u(\eta-\eta_0)$ is the unit step function which is defined as:

$$\begin{cases}u=1 & \text{for } \eta>\eta_0\\ u=0 & \text{for } \eta<\eta_0\end{cases}$$

This implies that the heating source assumes $S=1$ for $0<\eta<\eta_0$ and $S=0$ for $\eta>\eta_0$.

2.3.2. Harmonic heating source

In this case, the heating source fluctuates in a harmonic manner as:

$$S(\eta)=1+\varepsilon\sin(\omega\eta)$$

where ε is the fluctuation amplitude and ω is the dimensionless angular velocity.

2.4. Solution methodology

Eqs. (10) and (11) are solved numerically using finite difference scheme. The finite difference method is based on the central and forward discretization in time domain. Eqs. (17) and (18) are solved using Laplace transformation technique. Closed form expressions are obtained for the dimensionless lattice temperature for the two heating sources. The solutions are given as:

2.4.1. Unit step heating source

In this case, the dimensionless lattice temperature is given as:

$$\theta(\eta) = \big(h(\eta) - u(\eta-\eta_0)h(\eta-\eta_0)\big) \tag{19}$$

with

$$h(\eta) = -\frac{C_4}{C_3^2} + \frac{C_4}{C_3}\eta + \frac{C_4}{C_3^2}e^{-C_3\eta}$$

2.4.2. Harmonic heating source

In this case, the dimensionless lattice temperature is given as:

$$\theta(\eta) = h(\eta) = -\frac{\varepsilon C_4}{\omega C_3} - \frac{\varepsilon\omega C_4}{(C_3^3 + C_3\omega^2)}e^{-C_3\eta} - \frac{\varepsilon\omega C_4}{(C_3^2\omega+\omega^3)}\sin(\omega\eta) - \frac{\varepsilon C_3 C_4}{(C_3^2\omega+\omega^3)}\cos(\omega\eta) \tag{20}$$

3. Results and discussion

The plate is made of lead with properties shown in Table 1. The following set of figures show the transient thermal behavior of the lumped slab under different operating conditions and for both types of heating sources.

The concern is focused on the validity of the constant thermal properties, C_e and C_L, assumption. For each heating source, two sets of figures are obtained. The first set gives a comparison between the slab behavior with variable and constant lattice thermal capacity while other properties, such as C_e and G, are held constant. The second set gives a comparison between the slab behavior with variable and constant electron gas thermal capacity while other properties, such as C_L and G, are held constant. The deviation in the lattice temperature is defined as

$$\text{Percentage deviation} = \left|\frac{(\theta_L)_{\text{variable}} - (\theta_L)_{\text{constant}}}{(\theta_L)_{\text{variable}}}\right| \times 100\%$$

where $(\theta_L)_{\text{variable}}$ indicates that the lattice temperature is estimated with one of the thermal properties (C_e or C_L) is taken variable while the other property is held constant. On the otherhand, $(\theta_L)_{\text{constant}}$ indicates that the lattice temperature is estimated with both thermal properties (C_e and C_L) are held constant. In both cases, G is held constant.

Fig. 1 shows the transient variation in the dimensionless lattice temperature with variable and constant lattice thermal capacity C_L using the unit step heating source while C_e and G are held constants. It is clear from this figure that the difference between the two cases is insignificant until one reaches the end of the pulse signal at $\eta_0 = 1.0$.

Fig. 2 shows the percentage deviation in θ_L between the variable and constant C_L cases. It is clear that the

Table 1
Lead thermophysical properties

Properties at 300 K	
Melting point [K]	601
ρ [kg·m^{-3}]	11340
C_P [J·kg^{-1}·K^{-1}]	129
K [W·m^{-1}·K^{-1}]	35.3
α [m^2·s^{-1}]	24×10^{-6}
C_e [J·m^{-3}·K^{-1}]	2.1×10^4
C_L [J·m^{-3}·K^{-1}]	1.5×10^6
G [W·m^{-3}·K^{-1}]	12.4×10^{16}

Property	Temperature [K]			
	100	200	400	600
K [W·m^{-1}·K^{-1})	39.7	36.7	34.0	31.4
C_P [J·kg^{-1}·K^{-1}]	118	125	132	142

a	b	c	d	γ [J·m^{-3}·K^{-2}]
1205035.0	1674.27	−3.74587	0.00348	70

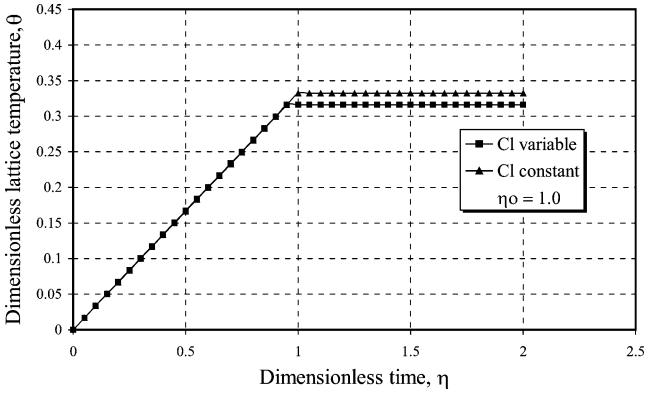

Fig. 1. Dimensionless lattice temperature versus dimensionless time using unit step heating source where C_e is constant ($\eta_0 = 1.0$).

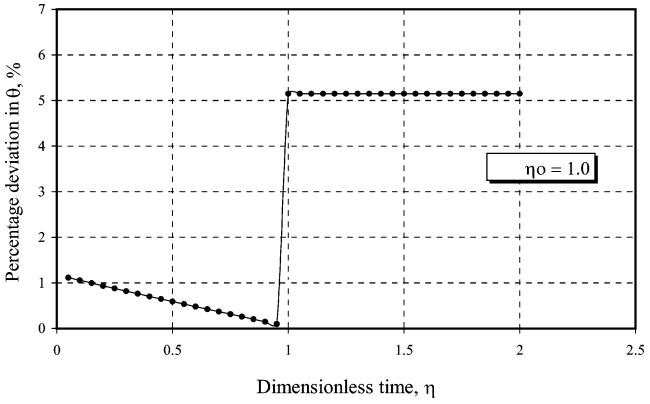

Fig. 2. Effect of C_L on the transient deviation in the lattice temperature using unit step heating source ($\eta_0 = 1.0$).

slab thermal behavior is not sensitive to the constant C_L assumption since the maximum deviation in θ_L between the two cases does not exceed 5%. It is clear from this figure that there is a sudden increase in the percentage deviation in θ_L which appears at the end of the unit step heating duration. In fact, this increase is not a large one and its maximum value does not exceed 5%. The reason why this sudden increase in the deviation appears at the end of the heating duration ($\eta_0 = 1.0$) is due to the fact that as the heating process proceeds, the lattice temperature increase then the error in assuming C_L constant increases and accumulates to appear at the end of the heating process and to maintain a fixed value after that.

Fig. 3 shows the transient variation in the dimensionless lattice temperature with variable and constant electron gas thermal capacity C_e using the unit step heating source while C_L and G are held constants. It is clear that the deviation between the two temperatures increases linearly until one reach the end of the pulse signal and then the deviation attains a fixed value.

Fig. 4 shows the transient variation in the dimensionless electron temperature with variable and constant electron gas thermal capacity C_e using the unit step heating source while C_L and G are held constants. It is clear that the deviation between the two temperatures increases linearly until one reach the end of the pulse signal and then the deviation attains a fixed value. From this figure we can see that the dimensionless electron temperature is higher than the dimensionless lattice temperature. This is predicted since the electron gas temperature varies over a wider temperature range as compared to the variation in the lattice temperature. The electron gas has smaller thermal capacity and it absorbs the incident radiative heat totally and directly and as a result, it attains much higher temperature as compared to the solid lattice.

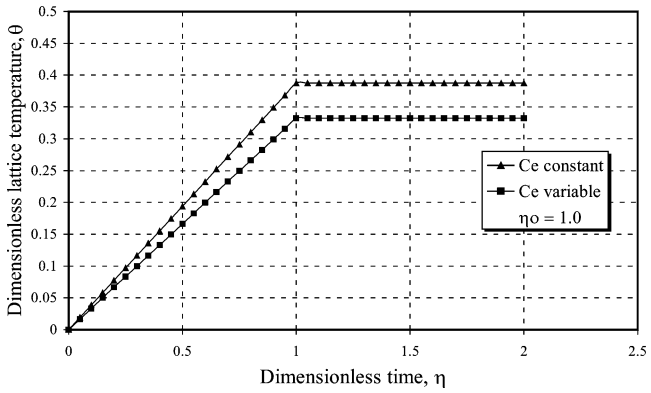

Fig. 3. Dimensionless lattice temperature versus dimensionless time using unit step heating source where C_L is constant ($\eta_0 = 1.0$).

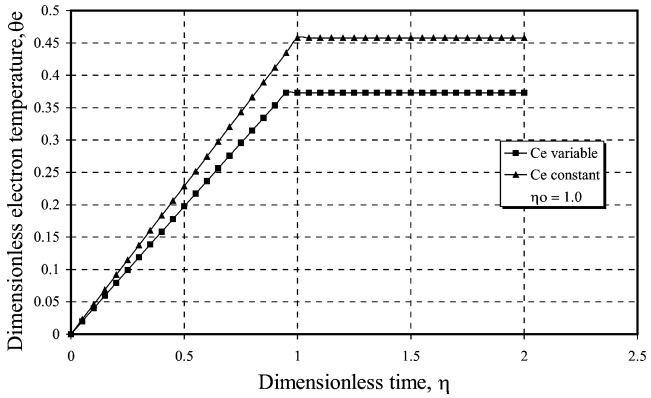

Fig. 4. Dimensionless electron temperature versus dimensionless time using unit step heating source where C_L is constant ($\eta_0 = 1.0$).

Fig. 5 shows the percentage deviation in θ_L between the variable and constant C_e cases. It is clear that the slab thermal behavior is very sensitive to the constant electron gas thermal capacity since the deviation in θ_L between the two cases is about 16%. It may be concluded that the parabolic microscopic heat conduction model is more sensitive to the variation in C_e as compared to the variation in C_L. This is predicted since the electron gas temperature varies over a wider temperature range as compared to the variation in the lattice temperature. The electron gas has smaller thermal capacity and it absorbs the incident radiative heat totally and directly and as a result, it attains much higher temperature as compared to the solid lattice.

Fig. 6 show the variation in the lattice temperature for a harmonic fluctuating heating source and for different

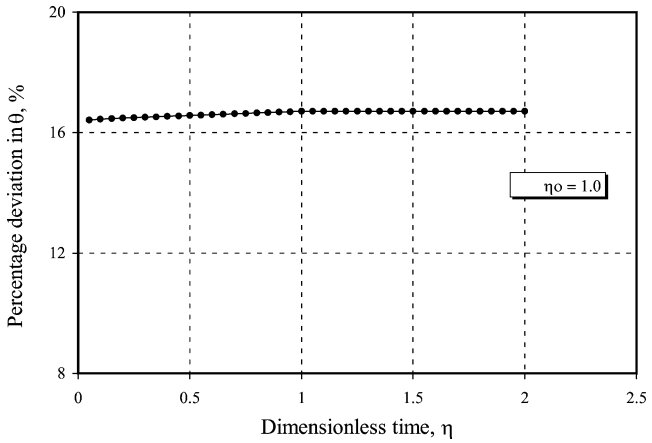

Fig. 5. Effect of C_e on the transient deviation in the lattice temperature using unit step heating source ($\eta_0 = 1.0$).

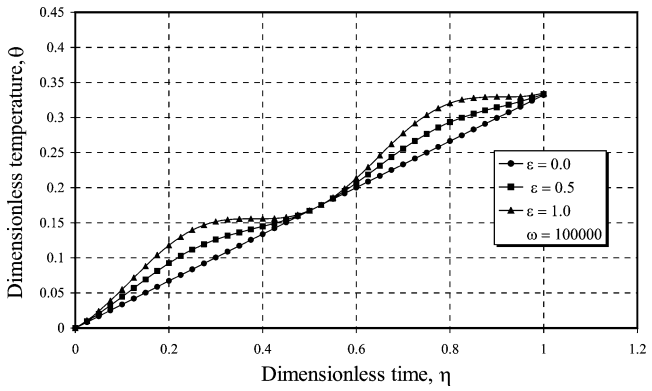

Fig. 6. Dimensionless lattice temperature versus dimensionless time using harmonic heating source where C_L is variable at different values of amplitude ($\omega = 100000$).

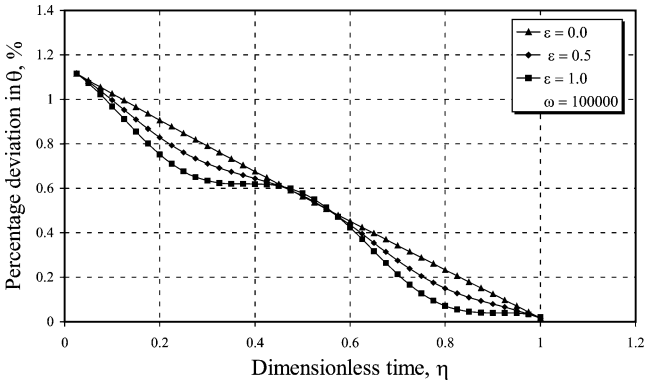

Fig. 7. Effect of C_L on the transient deviation in the lattice temperature using harmonic heating source at different values of amplitude ($\omega = 100000$).

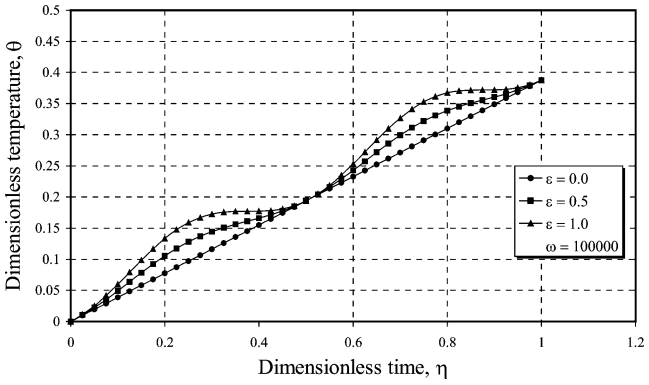

Fig. 8. Dimensionless lattice temperature versus dimensionless time using harmonic heating source where C_e is constant at different values of amplitude ($\omega = 100000$).

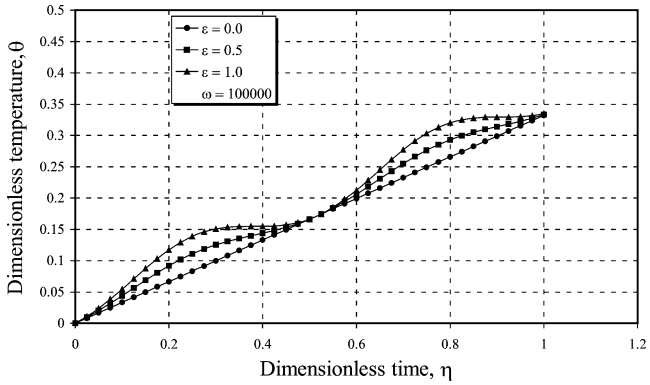

Fig. 9. Dimensionless lattice temperature versus dimensionless time using harmonic heating source where C_e is variable at different values of amplitude ($\omega = 100000$).

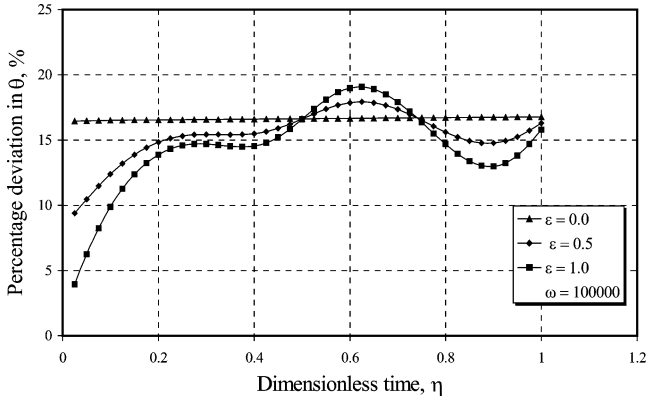

Fig. 10. Effect of C_e on the transient deviation in the lattice temperature using harmonic heating source at different values of amplitude ($\omega = 100000$).

fluctuation amplitudes ε. This figure obtained with variable C_L and C_e and G is held constants.

Fig. 7 shows the deviation in θ_L between the two cases and at different fluctuating amplitudes ε. It is clear that the deviation is very small since it does not exceed 1%. One may conclude that the slab behavior is not sensitive to the constant C_L assumption especially under harmonic fluctuating heating source. In the unit step heating source, this maximum deviation is found to be 5%.

Figs. 8 and 9 show the variation in the lattice temperature for a harmonic fluctuating heating source and for different fluctuation amplitudes ε. Fig. 8 is obtained with constant C_e while Fig. 9 is obtained with variable C_e and in both figures C_L and G are held constants.

Fig. 10 shows the deviation in θ_L between the two cases and at different fluctuations amplitudes ε. It is clear from this figure that the deviation is significant and may reach a value of 19%. This implies that the slab is very sensitive to the variation in the electron gas thermal capacity C_e. The sensitivity of the slab thermal behavior for the variation in C_e under fluctuating heating source is higher than that under unit step heating source. Table 2 summarize these results for both cases.

It worth mentioning here, that Table 2 compares among the maximum deviation in θ_L based on the assumption of constant or variable C_e and C_L and for the two heating sources. This maximum deviation may appear at any time. In case of unit step heating this maximum deviation appears at almost $\eta \approx \eta_0$ and after that maintains a fixed value. For harmonic heating this maximum deviation appears at $\eta < \eta_0$. This implies that, it is not fair to compare between the instantaneous deviation in θ_L since such a comparison give wrong indication. In general, if one interested in tracing the instantaneous deviation, then he has to return to the Figs. 2, 4, 7, and 10.

Table 2
Maximum percentage deviation in θ_L

	Type of heat source	
	Unit step	Harmonic
C_e constant	16.71%	19.10%
C_L constant	5.15%	1.11%

4. Concluding remarks

The validity of assuming constant total thermal capacity properties C_e and C_L in the parabolic microscopic heat

conduction model is examined for two types of volumetric heating sources. These types are the unit step and the harmonic fluctuating heating sources. For each heating type, two cases are considered. The first case assumes C_L variable while C_e and G are held constants and the second case assumes C_e variable while C_L and G are held constants. The results of these two cases are compared with the results of a basic case, which assumes C_e, C_L and G constants. The deviations between the results of each case and that of the basic case are estimated. Table 2 summarizes these results by focusing on the maximum deviation. It is concluded that the slab thermal behavior is more sensitive to the variation in C_e as compared to the variation in C_L. Also, it is concluded that this sensitivity regarding C_e is higher in the harmonic type heating source. The values of ω and η_0 are estimated based on practical values used in the literature.

References

[1] D.Y. Tzou, Macro-to-Microscale Heat Transfer—The Lagging Behavior, Taylor and Francis, New York, 1997, pp. 1–64.
[2] T.Q. Qiu, C.L. Tien, Short-pulse laser heating on metals, Internat. J. Heat Mass Transfer 35 (1992) 719–726.
[3] T.Q. Qiu, C.L. Tien, Heat transfer mechanism during short-pulse laser heating of metals, ASME J. Heat Transfer 115 (1993) 835–841.
[4] S.L. Anisimov, B.L. Kapeliovich, T.L. Perelman, Electron emission from metal surfaces exposed to ultra-short laser pulses, Soviet Phys. JETP 39 (1974) 375–377.
[5] J.G. Fujimoto, J.M. Liu, E.P. Ippen, Femtosecond laser interaction with metallic tungsten and non-equilibrium electron and lattice temperature, Phys. Rev. Lett. 53 (1984) 1837–1840.
[6] D.Y. Tzou, A unified approach for heat conduction from macro-to-microscales, J. Heat Transfer 117 (1995) 8–16.
[7] M.A. Al-Nimr, V.S. Arpaci, The thermal behavior of thin metal films in the hyperbolic two-step model, Internat. J. Heat Mass Transfer 43 (2000) 2021–2028.
[8] M.A. Al-Nimr, V.S. Arpaci, Picosecond thermal pulses in thin metal films, J. Appl. Phys. 85 (5) (1999) 2517–2521.
[9] M.A. Al-Nimr, S. Masoud, Nonequilibrium laser heating of metal films, J. Heat Transfer 119 (1997) 188–190.
[10] M.A. Al-Nimr, Heat transfer mechanisms during short-duration laser heating of thin metal films, Internat. J. Thermophys. 18(5) (1997) 1257–1268.
[11] M.A. Al-Nimr, O.M. Haddad, V.S. Arpaci, Thermal behavior of metal films—A hyperbolic two-step model, Heat Mass Transfer 35 (1999) 459–464.
[12] T.Q. Qiu, C.L. Tien, Femtosecond laser heating of multi-layered metals—I. Analysis, Internat. J. Heat Mass Transfer 37 (1994) 2789–2797.
[13] S. Kumar, M. Mitra, Microscale aspects of thermal radiation transport and laser applications, Adv. Heat Transfer 33 (1999) 187–294.
[14] C. Kittel, Introduction to Solid State Physics, seventh ed., Wiley, New York, 1996.